11th AIAA/ISSMO Multidisciplinary Analysis and Optimization Conference
6 - 8 September 2006, Portsmouth, Virginia

AIAA 2006-7000

Reliability-Based Design Optimization for Shape Design of Compliant Micro-Electro-Mechanical Systems

B. M. Adams*, M. S. Eldred†, and J. W. Wittwer‡
Sandia National Laboratories§, Albuquerque, NM 87185

Reliability methods are probabilistic algorithms for quantifying the effect of uncertainties on response metrics of interest. In particular, they compute approximate response function distribution statistics (probability, reliability, and response levels) based on specified probability distributions for input random variables. In conjunction with simulation software, these reliability analysis methods may be employed within reliability-based design optimization (RBDO) algorithms for designing systems subject to probabilistic performance criteria. In this paper, RBDO methods are compared and their effectiveness demonstrated by application to design optimization of microelectromechanical systems (MEMS), devices for which uncertainties in material properties and geometry affect performance and reliability. A new tapered beam topology for a fully compliant bistable mechanism is presented and its geometry optimized with RBDO to reliably achieve a specified actuation force, while simultaneously reducing predicted force variability due to material properties and manufacturing. The optimal designs specified by these optimization processes are predicted to be reliable, but also more robust to manufacturing process variations. Software-based MEMS design illustrates challenges faced when applying RBDO methods in engineering contexts.

I. Introduction

Pre-fabrication design optimization of microelectromechanical systems (MEMS) is an important emerging application of uncertainty quantification (UQ) and reliability-based design optimization (RBDO). Typically crafted of silicon, polymers, metals, or a combination thereof, MEMS serve as micro-scale sensors, actuators, switches, and machines with applications including robotics, biology and medicine, automobiles, RF electronics, and optical displays.[1] Design optimization of these devices is crucial due to high cost and long fabrication times. Uncertainty in the micromachining and etching processes used to manufacture MEMS can lead to large uncertainty in the behavior of the finished products. RBDO, coupled with computational mechanics models of MEMS, offers a means to quantify this uncertainty and determine a priori the most reliable design that meets performance criteria.

Uncertainty and sensitivity analysis techniques[2,3] that predate modern reliability methods have historically been used to understand variability in systems and these have natural application to MEMS. Recently, Monte Carlo and robust optimization techniques have been explored in this context as well.[4] These tools analyze the expected performance variability or robustness for a particular design.

Reliability methods are probabilistic algorithms for quantifying the effect of input uncertainties on response metrics of interest. In particular, they perform UQ by computing approximate response function distribution statistics based on specified probability distributions for input random variables. These response

*Limited Term Member of Technical Staff, Optimization and Uncertainty Estimation Department, MS-0370, Member AIAA.
†Principal Member of Technical Staff, Optimization and Uncertainty Estimation Department, MS-0370, Associate Fellow AIAA.
‡Senior Member of Technical Staff, MEMS Devices and Reliability Physics, MS-1310.
§Sandia is a multiprogram laboratory operated by Sandia Corporation, a Lockheed Martin Company, for the United States Department of Energy's National Nuclear Security Administration under Contract DE-AC04-94AL85000.

statistics include mean, standard deviation, and cumulative or complementary cumulative distribution function (CDF/CCDF) pairings of response levels and either probability or reliability levels. These methods are often more efficient at computing statistics in the tails of the response distributions (events with low probability) than sampling-based approaches because the number of samples required to resolve a low probability can be prohibitive. Thus, these methods, as their name implies, are often used in a reliability context for assessing the probability of failure of a system when confronted with an uncertain environment.

Classical reliability analysis methods include Mean-Value First-Order Second-Moment (MVFOSM), First-Order Reliability Method (FORM), and Second-Order Reliability Method (SORM).[5] More recent methods seek to improve the efficiency of FORM analysis through limit state approximations, including the local and multipoint approximations of Advanced Mean Value methods (AMV/AMV+)[6] and Two-point Adaptive Nonlinearity Approximation-based methods (TANA),[7,8] respectively. Each of the FORM-based methods can be employed for "forward" or "inverse" reliability analysis through the reliability index approach (RIA) or performance measure approach (PMA), respectively.[9]

The capability to assess reliability is broadly useful within a design optimization context, and reliability-based design optimization methods are popular approaches for designing systems while accounting for uncertainty. RBDO approaches may be broadly characterized as bi-level (in which the reliability analysis is nested within the optimization),[10] sequential (in which iteration occurs between optimization and reliability analysis),[11,12] or unilevel (in which the design and reliability searches are combined into a single optimization).[13] Bi-level RBDO methods are simple and general-purpose, but can be computationally demanding. Sequential and unilevel methods seek to reduce computational expense by breaking the nested relationship through the use of iterated/surrogate or simultaneous approaches, respectively.

A compelling technical advantage of microsystems is that, like integrated circuits, they can be batch fabricated for high volume applications. Designing MEMS that are less sensitive to manufacturing process variations results in higher yield of reliable devices. Recognizing the importance of designing reliable and robust systems, researchers have coupled uncertainty analysis and reliability methods with design optimization for MEMS. Many have considered design problems similar to those presented in this paper. For example, Liu, et al., sought designs robust to width variations[14] and Mawardi and Pitchumanu applied robust optimization to resonators.[15] Compliant MEMS were also explored by Maute and Frangopol who investigated topology optimization with reliability-based design methods.[16] Wittwer, et al., united modern uncertainty analysis, model validation, and robust optimization techniques in a comprehensive design method accounting for process uncertainties.[17]

This paper explores a variety of algorithms for performing reliability analysis. In particular, forward and inverse reliability analyses are described, including variations in limit state approximation, probability integration, Hessian approximation, and most probable point search algorithms. These uncertainty quantification capabilities are then used as a foundation for exploring RBDO formulations. The algorithms described are implemented in the DAKOTA software suite,[18] an open-source software framework for design and performance analysis of large-scale computational models on high performance computers, which couples with finite element-based simulations to generate design results for the MEMS devices of interest.

Sections II and III describe the reliability and RBDO algorithms, respectively. Section IV demonstrates their application to a compliant bistable micromechanism. Section V provides concluding remarks and indicates future directions.

II. Reliability Method Formulations

A. Mean Value

The Mean Value method (MV, also known as MVFOSM)[5] is the simplest, least-expensive reliability method because it estimates the response means, response standard deviations, and all CDF/CCDF response-probability-reliability levels from a single evaluation of response functions and their gradients at the uncertain variable means. This approximation can have acceptable accuracy when the response functions are nearly linear and their distributions are approximately Gaussian, but can have poor accuracy in other situations. The expressions for approximate response mean μ_g, approximate response standard deviation σ_g, response target to approximate probability/reliability level mapping ($\bar{z} \rightarrow p, \beta$), and probability/reliability target to

approximate response level mapping ($\bar{p}, \bar{\beta} \rightarrow z$) are

$$\mu_g = g(\mu_{\mathbf{x}}) \tag{1}$$

$$\sigma_g = \sum_i \sum_j Cov(i,j) \frac{dg}{dx_i}(\mu_{\mathbf{x}}) \frac{dg}{dx_j}(\mu_{\mathbf{x}}) \tag{2}$$

$$\beta_{cdf} = \frac{\mu_g - \bar{z}}{\sigma_g} \tag{3}$$

$$\beta_{ccdf} = \frac{\bar{z} - \mu_g}{\sigma_g} \tag{4}$$

$$z = \mu_g - \sigma_g \bar{\beta}_{cdf} \tag{5}$$

$$z = \mu_g + \sigma_g \bar{\beta}_{ccdf} \tag{6}$$

respectively, where $\mathbf{x}$ are the uncertain values in the space of the original uncertain variables ("x-space"), with μ denoting mean, $g(\mathbf{x})$ is the response function for which probability-response level pairs are needed, and β_{cdf} and β_{ccdf} are the CDF and CCDF reliability indices, respectively.

With the introduction of second-order limit state information, Mean-Value Second-Order Second-Moment (MVSOSM) calculates a second-order mean as

$$\mu_g = g(\mu_{\mathbf{x}}) + \frac{1}{2} \sum_i \sum_j Cov(i,j) \frac{d^2 g}{dx_i dx_j}(\mu_{\mathbf{x}}) \tag{7}$$

This is commonly combined with a first-order variance (Eq. 2), since second-order variance involves higher order distribution moments (skewness, kurtosis)[5] which are often unavailable. For MPP searches informed by Hessian information (described in Section II.B), the MVSOSM second-order mean (Eq. 7) can be used to calculate response means.

The first-order CDF probability $p(g \leq z)$, first-order CCDF probability $p(g > z)$, β_{cdf}, and β_{ccdf} are related to one another through

$$p(g \leq z) = \Phi(-\beta_{cdf}) \tag{8}$$

$$p(g > z) = \Phi(-\beta_{ccdf}) \tag{9}$$

$$\beta_{cdf} = -\Phi^{-1}(p(g \leq z)) \tag{10}$$

$$\beta_{ccdf} = -\Phi^{-1}(p(g > z)) \tag{11}$$

$$\beta_{cdf} = -\beta_{ccdf} \tag{12}$$

$$p(g \leq z) = 1 - p(g > z) \tag{13}$$

where $\Phi()$ is the standard normal cumulative distribution function. A common convention in the literature is to define g in such a way that the CDF probability for a response level z of zero (i.e., $p(g \leq 0)$) is the response metric of interest. The formulations in this paper are not restricted to this convention and are designed to support CDF or CCDF mappings for general response, probability, and reliability level sequences.

B. MPP Search Methods

Other reliability methods solve an equality-constrained nonlinear optimization problem to compute a most probable point (MPP) and then integrate about this point to compute probabilities. The MPP search is performed in uncorrelated standard normal space ("u-space") since it simplifies the probability integration: the distance of the MPP from the origin has the meaning of the number of input standard deviations separating the mean response from a particular response threshold. The transformation from correlated non-normal distributions (x-space) to uncorrelated standard normal distributions (u-space) is denoted as $\mathbf{u} = T(\mathbf{x})$ with the reverse transformation denoted as $\mathbf{x} = T^{-1}(\mathbf{u})$. These transformations are nonlinear in general, and possible approaches include the Rosenblatt,[19] Nataf,[20] and Box-Cox[21] transformations. The nonlinear transformations may also be linearized, and common approaches for this include the Rackwitz-Fiessler[22] two-parameter equivalent normal and the Chen-Lind[23] and Wu-Wirsching[24] three-parameter equivalent normals. The results in this paper employ the Nataf nonlinear transformation which occurs in the following two steps.

To transform between the original correlated x-space variables and correlated standard normals ("z-space"), the CDF matching condition is used:

$$\Phi(z_i) = F(x_i) \tag{14}$$

where $F()$ is the cumulative distribution function of the original probability distribution. Then, to transform between correlated z-space variables and uncorrelated u-space variables, the Cholesky factor $\mathbf{L}$ of a modified correlation matrix is used:

$$\mathbf{z} = \mathbf{L}\mathbf{u} \tag{15}$$

where the original correlation matrix for non-normals in x-space has been modified to represent the corresponding correlation in z-space.[20]

The forward reliability analysis algorithm of computing CDF/CCDF probability levels p or reliability levels β for specified response levels $\bar{z}$ is called the reliability index approach (RIA), and the inverse reliability analysis algorithm of computing response levels z for specified CDF/CCDF probability levels $\bar{p}$ or reliability levels $\bar{\beta}$ is called the performance measure approach (PMA).[9] The differences between the RIA and PMA formulations appear in the objective function and equality constraint formulations used in the MPP searches. For RIA, the MPP search for achieving the specified response level $\bar{z}$ is formulated as

$$\begin{aligned} \text{minimize} \quad & \mathbf{u}^T\mathbf{u} \\ \text{subject to} \quad & G(\mathbf{u}) = \bar{z} \end{aligned} \tag{16}$$

and for PMA, the MPP search for achieving the specified reliability/probability level $\bar{\beta}, \bar{p}$ is formulated as

$$\begin{aligned} \text{minimize (or maximize)} \quad & G(\mathbf{u}) \\ \text{subject to} \quad & \mathbf{u}^T\mathbf{u} = \bar{\beta}^2 \end{aligned} \tag{17}$$

where $\mathbf{u}$ is a vector centered at the origin in u-space and $G(\mathbf{u}) = g(\mathbf{x})$ by definition. In the RIA case, the optimal MPP solution $\mathbf{u}^*$ defines the reliability index from $\beta = \pm\|\mathbf{u}^*\|_2$, which in turn defines the CDF/CCDF probabilities (using Eqs. 8 and 9 in the case of first-order integration). The sign of β is defined by

$$\begin{aligned} G(\mathbf{u}^*) > G(\mathbf{0}) &: \beta_{cdf} < 0, \beta_{ccdf} > 0 \\ G(\mathbf{u}^*) < G(\mathbf{0}) &: \beta_{cdf} > 0, \beta_{ccdf} < 0 \end{aligned}$$

where $G(\mathbf{0})$ is the median limit state response computed at the origin in u-space (where $\beta_{cdf} = \beta_{ccdf} = 0$ and first-order $p(g \leq z) = p(g > z) = 0.5$). In the PMA case, the minimization or maximization of $G(\mathbf{u})$ is similarly determined by $\bar{\beta}$:

$$\begin{aligned} \bar{\beta}_{cdf} < 0, \bar{\beta}_{ccdf} > 0 &: \text{maximize } G(\mathbf{u}) \\ \bar{\beta}_{cdf} > 0, \bar{\beta}_{ccdf} < 0 &: \text{minimize } G(\mathbf{u}) \end{aligned}$$

and the limit state at the MPP ($G(\mathbf{u}^*)$) defines the desired response level result.

There are a variety of algorithmic variations that can be explored within RIA/PMA reliability analysis including limit state approximations, probability integrations, warm starting approaches, Hessian approximations, and MPP search algorithm selections.[25,26] The results in this paper come from either directly optimizing without approximating the limit state $G(u)$ (FORM), or optimizing the AMV^2+ approximation,[26] where a second-order Taylor series model of the limit state is used and updated as the optimization progresses with rank one updates to the Hessian and new expansions about each candidate MPP. When the specified response metrics or constraints include probabilities $\bar{p}$, they must be calculated by integrating around the most probable point in u-space. First-order integration methods directly use Eqs. 8 and 9 and second-order integration methods are discussed in Ref. 26, including the Breitung correction, which uses principal curvatures κ_i of the limit state function to better inform the integration. First-order integrations are employed for the probability formulation RBDO process presented in Section IV, however the probabilities about the resulting converged MPPs are verified using second-order integrations (SORM) with full finite-difference Hessians.

III. Reliability-Based Design Optimization

Reliability-based design optimization (RBDO) methods are used to perform design optimization accounting for reliability metrics. The reliability analysis capabilities described in Section II provide a rich foundation for exploring a variety of RBDO formulations. In Ref. 25, Eldred, et al., investigated bi-level, fully-analytic bi-level, and first-order sequential RBDO approaches employing underlying first-order reliability assessments. In Ref. 26, Eldred and Bichon investigated fully-analytic bi-level and second-order sequential RBDO approaches employing underlying second-order reliability assessments.

In bi-level (nested) RBDO, the simplest and most direct RBDO approach (and that employed in this paper), an optimization algorithm is used to minimize over design variables $\mathbf{d}$ an objective function subject to constraints, where each of these include dependence on design variables and/or statistics generated by reliability analysis. For each design iterate $\mathbf{d}$, evaluation of the statistics requires a full probability/reliability analysis over the uncertain variables $\mathbf{x}$. Thus bi-level RBDO involves a nesting of two distinct levels of optimization within each other, one at the design level and one at the MPP search level.

Since an RBDO problem will typically specify both the $\bar{z}$ level and either the $\bar{p}$ or $\bar{\beta}$ level, one can use either the RIA or the PMA formulation for the UQ portion and then constrain the result in the design optimization portion. In particular, RIA reliability analysis (Eq. 16) maps a specified response level $\bar{z}$ to p or β, so RIA RBDO constrains p or β:

$$\begin{aligned} \text{minimize} \quad & f(\mathbf{d}, \mathbf{x}) \\ \text{subject to} \quad & \beta(\mathbf{d}) \geq \bar{\beta} \\ \text{or} \quad & p(\mathbf{d}) \leq \bar{p} \end{aligned} \tag{18}$$

And PMA reliability analysis (Eq. 17) maps a desired probability $\bar{p}$ or reliability $\bar{\beta}$ to z, so PMA RBDO constrains z:

$$\begin{aligned} \text{minimize} \quad & f(\mathbf{d}, \mathbf{x}) \\ \text{subject to} \quad & z(\mathbf{d}) \geq \bar{z} \end{aligned} \tag{19}$$

where $z \geq \bar{z}$ is used as the RBDO constraint for a cumulative failure probability (failure defined as $z \leq \bar{z}$) but $z \leq \bar{z}$ would be used as the RBDO constraint for a complementary cumulative failure probability (failure defined as $z \geq \bar{z}$). While DAKOTA can solve these simple inequality-constrained RBDO formulations, it also supports general optimization under uncertainty mappings[27] which allow flexible use of statistics within multiple objectives, inequality constraints, and equality constraints.

In solving an optimization problem, many algorithms require derivatives of the objective function and constraints with respect to $\mathbf{d}$. An important performance enhancement for bi-level methods uses sensitivity analysis to compute the design gradients of probability, reliability, and response levels, relying on the analytic relationship between derivatives of the response function g and reliability metrics. In particular, when design variables are separate from the uncertain variables (i.e., they are not parameters of uncertain variable distributions), then the following first-order expressions may be used:[10, 28, 29]

$$\nabla_{\mathbf{d}} z = \nabla_{\mathbf{d}} g \tag{20}$$

$$\nabla_{\mathbf{d}} \beta_{cdf} = \frac{1}{\parallel \nabla_{\mathbf{u}} G \parallel} \nabla_{\mathbf{d}} g \tag{21}$$

$$\nabla_{\mathbf{d}} p_{cdf} = -\phi(-\beta_{cdf}) \nabla_{\mathbf{d}} \beta_{cdf} \tag{22}$$

where it is evident from Eqs. 12 and 13 that $\nabla_{\mathbf{d}} \beta_{ccdf} = -\nabla_{\mathbf{d}} \beta_{cdf}$ and $\nabla_{\mathbf{d}} p_{ccdf} = -\nabla_{\mathbf{d}} p_{cdf}$. If second-order integration is used to calculate p from β, Eq. 22 must be expanded to include a curvature correction.[26] Even when $\nabla_{\mathbf{d}} g$ is estimated numerically, Eqs. 20–22 can be used to avoid numerical differencing across full reliability analyses to obtain design derivatives.

When the design variables are distribution parameters of the uncertain variables, $\nabla_{\mathbf{d}} g$ is expanded with the chain rule and Eqs. 20 and 21 become

$$\nabla_{\mathbf{d}} z = \nabla_{\mathbf{d}} \mathbf{x} \nabla_{\mathbf{x}} g \tag{23}$$

$$\nabla_{\mathbf{d}} \beta_{cdf} = \frac{1}{\parallel \nabla_{\mathbf{u}} G \parallel} \nabla_{\mathbf{d}} \mathbf{x} \nabla_{\mathbf{x}} g \tag{24}$$

where the design Jacobian of the transformation ($\nabla_{\mathbf{d}}\mathbf{x}$) may be obtained analytically for uncorrelated $\mathbf{x}$ or semi-analytically for correlated $\mathbf{x}$ ($\nabla_{\mathbf{d}}\mathbf{L}$ is evaluated numerically) by differentiating Eqs. 14 and 15 with respect to the distribution parameters. Eq. 22 remains the same as before. For this design variable case, all required information for the sensitivities is available from the MPP search.

Since Eqs. 20–24 are derived using the Karush-Kuhn-Tucker (KKT) conditions for a converged MPP, they are appropriate for RBDO using AMV+, TANA, FORM, and SORM, but not for RBDO using MVFOSM, MVSOSM, or AMV.

An alternative RBDO approach is the sequential approach, in which additional efficiency is sought by breaking the nested relationship of the MPP and design searches. The general concept is to iterate between optimization and uncertainty quantification, updating the optimization goals based on the most recent probabilistic assessment results. This update may be based on safety factors[11] or other approximations.[12]

A particularly effective approach for updating the optimization goals is to use the $p/\beta/z$ sensitivity analysis of Eqs. 20–24 in combination with local surrogate models.[30] In Refs. 25 and 26, first-order and second-order Taylor series approximations are explored. Surrogate models are used for both the objective function and the constraints, although the use of surrogates for probabilistic functions alone is sufficient to remove the nesting. When surrogate models are employed, a trust-region model management framework[31] can be used to adaptively manage the extent of the approximations and ensure convergence of the RBDO process. Further, when using second-order approximations, the design Hessians can be efficiently approximated with quasi-Newton updates.

IV. Application to MEMS Bistable Mechanism

In this section, the reliability analysis and design algorithms described in Sections II and III are applied to bistable microelectromechanical systems.

MEMS bistable mechanisms toggle between two stable positions, making them useful as micro switches, relays, and nonvolatile memory. In particular, the focus here is on shape optimization of compliant bistable mechanisms, where instead of mechanical joints, material elasticity and geometry enable the bistability of the mechanism.[32–34] Figure 1 contains an electron micrograph of a MEMS compliant bistable mechanism in its second stable position. The first stable position is the as-fabricated position. One achieves transfer between stable states by applying force to the center shuttle via a thermal actuator, electrostatic actuator, or other means to move the shuttle past an unstable equilibrium.

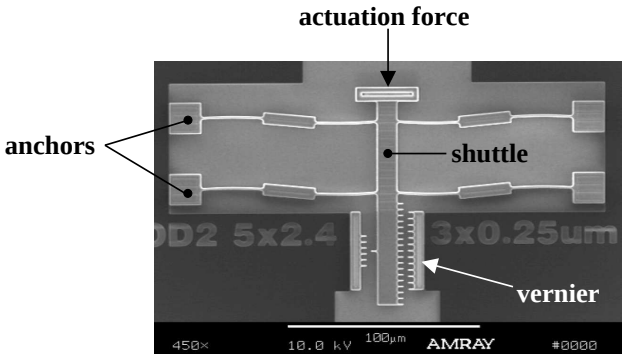

Figure 1. Scanning electron micrograph of a MEMS bistable mechanism in its second stable position. The attached vernier provides position measurements.[35]

Bistable switch actuation characteristics depend on the relationship between actuation force and shuttle displacement for the manufactured switch. Figure 2 contains a schematic of a typical force–displacement curve for a bistable mechanism. The switch characterized by this curve has three equilibria: E_1 and E_3 are stable equilibria whereas E_2 is an unstable equilibrium (arrows indicate stability). A device with such a force–displacement curve could be used as a switch or actuator by setting the shuttle to position E_3 as shown in Figure 1 (requiring large actuator force F_{max}) and then actuating by applying the comparably small force F_{min} in the opposite direction to transfer back through E_2 toward the equilibrium E_1. One could utilize this force profile to complete a circuit by placing a switch contact near the displaced position corresponding to maximum (closure) force as illustrated. Repeated actuation of the switch relies on being able to reset it

with actuation force F_{max}.

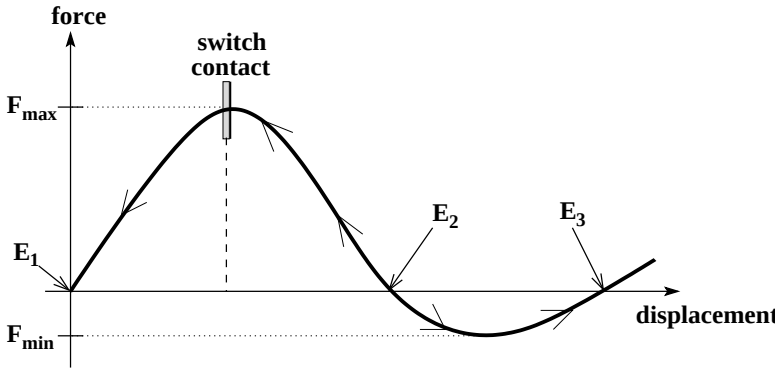

Figure 2. Schematic of force–displacement curve for bistable MEMS mechanism. The arrows indicate stability of equilibria E_1 and E_3 and instability of E_2.

The device design considered in this paper is similar to that in the electron micrograph in Figure 1, for which design optimization has been previously considered,[34] as has robust design under uncertainty with mean value methods.[17] The primary structural difference in the present design is the tapering of the legs, shown schematically in Figure 3. This topology is a cross between the fully compliant bistable mechanism

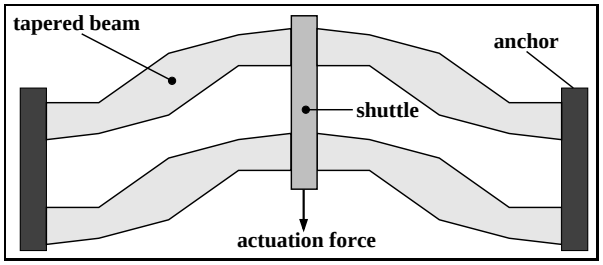

Figure 3. Schematic of a tapered beam bistable mechanism in as-fabricated position (not to scale).

reported in Ref. 34 and the thickness-modulated curved beam in Ref. 36. As described in the optimization problem below, this tapered geometry offers many degrees of freedom for design.

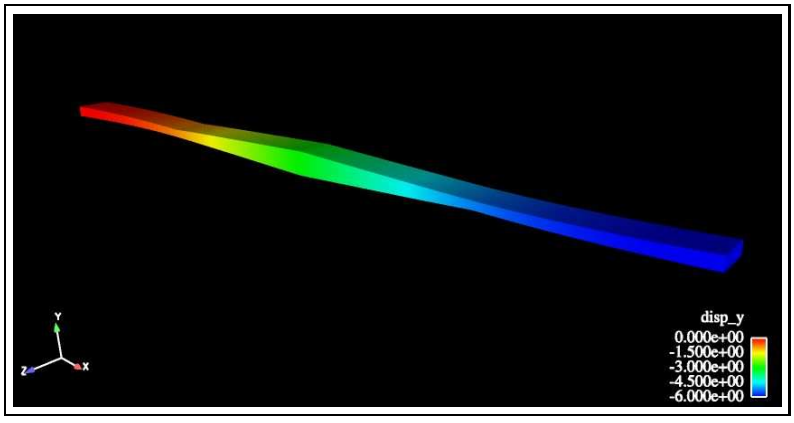

Figure 4. Scale drawing of tapered beam leg for bistable mechanism.

An appropriately designed bistable switch actuates predictably with prescribed force $\bar{F}_{min}$ and is robust to fabrication variations. The switch investigated here is subject to the following design criteria:

- reliably achieves specified actuation force $\bar{F}_{min} = -5\,\mu N$;
- is bistable ($F_{max} > 0$ and $F_{min} < 0$);

- attains at least $50\,\mu N$ force F_{max} at switch contact to reduce electrical contact resistance, but requires no more than $150\,\mu N$ actuation force to set;
- unstable point E_2 occurs at no more than $8\,\mu m$ (limited by the actuator displacement); and
- maximum stress no more than 1200 MPa.

The maximum stress constraint is relaxed to 3000 MPa for the analysis and optimization conducted here, to allow for the stress concentration resulting from the particular numerical simulation used. The actual device has stress-reducing fillets, which in a more rigorous analysis would be modeled and therefore accounted for during design optimization. The force–displacement profile of a compliant bistable MEMS device is highly sensitive to design geometry, so one can vary manufactured geometry to achieve these design criteria.

A. RBDO problem formulation

Figure 4 shows a scale drawing of one tapered beam leg (one quarter of the full switch system). A single leg is approximately 100 μm wide and 5–10 μm tall and is parametrized by the 13 design variables shown in Figure 5, including widths and lengths of beam segments as well as angles between segments. For simulation, a symmetry boundary condition allowing only displacement in the y direction is applied to the right surface ($x = 0$) and a fixed displacement condition is applied to the left surface. With appropriate scaling of reaction force (to account for device thickness and number of legs), these allow the quarter model to reasonably represent the full four-leg switch system.

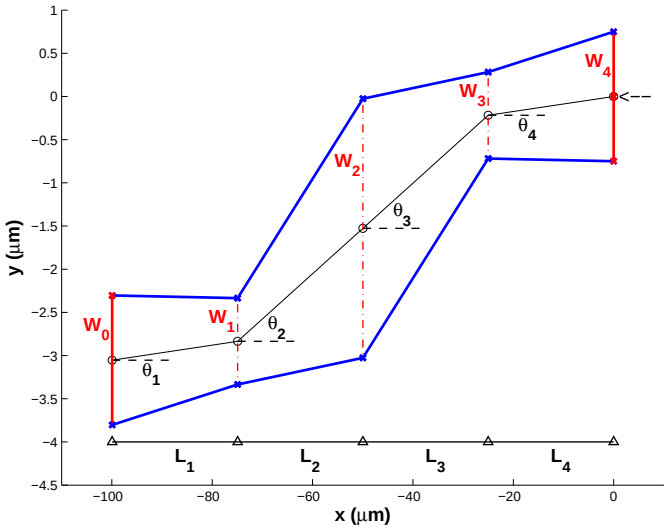

Figure 5. Design parameters for the tapered-beam fully-compliant bistable mechanism (geometry not to scale). Displacement is applied in the negative y direction at the right face ($x = 0$), while at the left face, a fixed displacement condition is enforced.

Due to manufacturing processes, fabricated geometry can deviate significantly from design-specified beam geometry. As a consequence of photo lithography and etching processes, fabricated in-plane geometry edges (contributing to widths and lengths) can be $0.1 \pm 0.08\,\mu m$ less than specified. This uncertainty in the manufactured geometry leads to substantial uncertainty in the positions of the stable equilibria and in the maximum and minimum force on the force–displacement curve. The manufactured thickness of the device is also uncertain, though this does not contribute as much to variability in the force–displacement behavior. Uncertain material properties such as Young's modulus and residual stress also influence the characteristics of the fabricated beam. For this application, two key uncertain variables are considered: ΔW (effect of edge bias, applied $\frac{\Delta W}{2}$ to each edge, yielding effective manufactured widths $W_i + \Delta W, i = 0, \ldots, 4$) and S_r (residual stress in the manufactured device), with distributions shown in Table 1.

Given the 13 geometric design variables $\mathbf{d} = [L_1, L_2, L_3, L_4, \theta_1, \theta_2, \theta_3, \theta_4, W_0, W_1, W_2, W_3, W_4]$ (subject to the bound constraints listed in Table 2) and the specified uncertain variables $\mathbf{x} = [\Delta W, S_r]$, we formulate two reliability-based design optimization problems to achieve a design that actuates reliably with 5 μN force. (In

Table 1. Uncertain variables $\mathbf{x} = [\Delta W, S_r]$ used in RBDO.

variable	mean (μ)	std. dev.	distribution
ΔW (width bias)	-0.2 μm	0.08	normal
S_r (residual stress)	-11 Mpa	4.13	normal

the following problem descriptions and results, units of force are μN and units of displacement (including equilibrium positions) are μm. The first formulation is reliability metric-based using the limit state

$$g(\mathbf{x}) = F_{min}(\mathbf{x}) \tag{25}$$

and failure is defined to be actuation force with magnitude less than 5.0 μN ($F_{min} > -5.0$). Reliability index $\beta_{ccdf} \geq 2$ is required. The RBDO problem utilizes the RIA $\bar{z} \rightarrow \beta$ approach (Eq. 18) with $\bar{z} = -5.0$:

$$\begin{array}{lrcrcl} \max & & & \mathrm{E}\left[F_{min}(\mathbf{d},\mathbf{x})\right] & & \\ \text{s.t.} & 2 & \leq & \beta_{ccdf}(\mathbf{d}) & & \\ & 50 & \leq & \mathrm{E}\left[F_{max}(\mathbf{d},\mathbf{x})\right] & \leq & 150 \\ & & & \mathrm{E}\left[E_2(\mathbf{d},\mathbf{x})\right] & \leq & 8 \\ & & & \mathrm{E}\left[S_{max}(\mathbf{d},\mathbf{x})\right] & \leq & 3000, \end{array} \tag{26}$$

although the PMA $\bar{\beta} \rightarrow z$ approach (Eq. 19) could also be used. The use of the F_{min} metric in both the objective function and the reliability constraint results in a powerful problem formulation, because in addition to yielding a design with specified reliability, it also produces a robust design. By forcing the expected value of F_{min} toward the -5.0 target while requiring two standard deviations of surety, the optimization problem favors designs with less variability in F_{min}. This renders the design performance less sensitive to uncertainties.

The second problem formulation seeks design variables $\mathbf{d}$ to maximize the probability of actuation force being in the desired interval $[-6.2, -5.0]$. For comparison with the previous reliability formulation, the interval is chosen such that the response level $F_{min} = -5.0$ deviates approximately 10% from the midpoint -5.6 of the interval. The optimization problem is:

$$\begin{array}{lrcrcl} \max & P(-6.2 & \leq & F_{min}(\mathbf{d},\mathbf{x}) & \leq & -5.0) \\ \text{s.t.} & 50 & \leq & \mathrm{E}\left[F_{max}(\mathbf{d},\mathbf{x})\right] & \leq & 150 \\ & & & \mathrm{E}\left[E_2(\mathbf{d},\mathbf{x})\right] & \leq & 8 \\ & & & \mathrm{E}\left[S_{max}(\mathbf{d},\mathbf{x})\right] & \leq & 3000. \end{array} \tag{27}$$

An equivalent alternative to this probability formulation directly incorporates the reliability metric β_{cdf} corresponding to response levels $\bar{z} = -6.2$ and $\bar{z} = -5.0$ in the optimization criterion:

$$\max \quad \beta_{cdf}^{(\bar{z}=-6.2)}(\mathbf{d}) - \beta_{cdf}^{(\bar{z}=-5.0)}(\mathbf{d}) \tag{28}$$

(subject to the same nonlinear constraints). This formulation defines failure as $F_{min} < -6.2$ or $F_{min} > -5.0$ and favors designs with the smallest probability of failure, however, the β statistic sometimes performs better than probability metrics in RBDO contexts.

The probability-based formulations in Eqs. 27 and 28 favor neither tail and yield robust designs by maximizing probability in a fixed interval. In contrast, the reliability formulation in Eq. 26 yields robust and reliable designs by constraining the right tail behavior of the output probability distribution while maximizing the distribution mean. An alternate casting of the RBDO problem that controls both distribution tails would retain the RIA-based reliability constraint $2 \leq \beta_{ccdf}$ from Eq. 26 and instead maximize the response level z corresponding to $\bar{\beta}_{ccdf} = -2$ (representing the left tail, calculated with PMA). Like Eq. 26, this combined RIA/PMA formulation would yield reliable and robust designs, however it is not explored numerically in this paper. Further studies are in progress to compare the effect of various problem formulations and algorithm selections.

Throughout design optimization, for each set of specified geometric design parameters and realizations of uncertain variables, we create and mesh the tapered beam geometry and then perform finite element

analysis to simulate the nonlinear elastic deformation of the beam through discrete displacement steps to produce a force–displacement curve. Maximum and minimum force values as well as displacement equilibria are determined from the curve. Maximum stress S_{max} is calculated as the maximum Von Mises stress over all nodes and all displacement steps. Finite element analysis is performed with Aria, a Galerkin finite element-based program for coupled-physics problems implemented in Sandia National Laboratories' SIERRA framework of multi-physics codes.[37] All switch simulations employ the quarter model (single beam) system described above, with appropriate boundary conditions and multipliers to recover the full system.

The optimization problem is solved by applying the DAKOTA software in a bi-level (nested) RBDO approach. The design variable optimization is performed by the DOT optimizer using the modified method of feasible directions (MMFD)[38] and, for each design iterate, a complete uncertainty/reliability analysis is performed with DAKOTA's reliability methods. We compare three reliability analysis methods for this MEMS application: (1) MVFOSM (no MPP search), (2) AMV^2+, and (3) FORM using a nonlinear interior point method to solve the MPP optimization subproblems. The latter two are advantaged by their ability to provide (semi-)analytic derivatives of reliability metrics with respect to design variables for the optimizer (see Section III), whereas the former must resort to numerical (finite difference) design derivatives due to the use of σ_g to compute β (for general distributions, analytic derivatives of Eq. 2 with respect to $\mathbf{d}$ are impractical to evaluate). Feasible initial iterates for the gradient-based MMFD were obtained using the hyper-rectangle sampling algorithm DIRECT.[39]

B. Numerical results

Results for the reliability problem formulation in Eq. 26 using the MVFOSM, AMV^2+, and FORM methods are presented in Table 2 and the optimal force–displacement curves are shown in Figure 6. Optimization with MVFOSM reliability analysis offers substantial improvement over the initial design, yielding a design with actuation force F_{min} nearer the -5.0 target and tight reliability constraint $\beta = 2$. However, since mean value analyses estimate reliability based solely on evaluations at the means of the uncertain variables, they can yield inaccurate reliability metrics in cases of nonlinearity or nonnormality. In this example, the actual reliability (verified with MPP-based methods) of the optimal MVFOSM-based design is only 1.804 (AMV^2+) or 1.707 (FORM); both less than the prescribed reliability $\beta \geq 2$. In this example, the additional computational expense incurred when computing the MPP via optimization may be justified.

Reliability-based design optimization with either the AMV^2+ or FORM methods for reliability analysis yield constraint-respecting optimal beam designs with significantly different geometries than MVFOSM. The MPP-based methods yield a more conservative value of F_{min} due to the improved estimation of β. Each of the three methods yields an improved design that respects the reliability constraint. The variability in F_{min} has been reduced from approximately 5.6 (initial) to 0.52 (MVFOSM design), 0.67 (AMV^2+ design), or 0.65 (FORM design) μN per (FORM verified) input standard deviation ($\frac{\mathrm{E}[F_{min}]-\bar{F}_{min}}{\beta}$), resulting in designs that are less sensitive to input uncertainties.

For the MVFOSM optimal design, the verified values of β calculated by AMV^2+ and FORM differ by 6%, illustrating a typical challenge engineering design problems pose to reliability analysis methods. Figure 7 displays the results of a parameter study for the metric $F_{min}(\mathbf{d}, \mathbf{x})$ as a function of the uncertain variables $\mathbf{x}$ for fixed design variables $\mathbf{d} = \mathbf{d}^*_M$ (the optimum from MVFOSM RBDO). Since the uncertain variables are both normal, the transformation to u-space used by AMV^2+ and FORM is linear, so the contour plot is scaled to a ± 3 standard deviation range in the native x-space. The relevant limit state for MPP searches, $g(\mathbf{x}) = F_{min}(\mathbf{x}) = -5.0$, is indicated by the dashed line. For some design variable sets $\mathbf{d}$ (not depicted), the limit state is relatively well-behaved in the range of interest and first-order probability integrations would be sufficiently accurate. For the design variable set $\mathbf{d}^*_M$ used to generate Figure 7, the limit state has significant nonlinearity, and thus demands more sophisticated probability integrations. The most probable points converged to by the AMV^2+ and FORM methods are denoted in Figure 7 by the plus sign and circle, respectively. While the distance from each point to the origin differs slightly (see verified β values in Table 2), there clearly exist multiple candidates for the most probable point $\mathbf{u}$ satisfying Eq. 16.

Another computational difficulty observed during design optimization of an earlier bistable mechanism design is simulation failure resulting from model evaluation at extreme values of physical and/or geometric parameters. For example, during an MPP search, edge bias ΔW might grow in magnitude into its left tail causing the effective width of the beam to shrink, possibly resulting in too flimsy a structure to simulate. In summary, highly nonlinear limit states, nonsmooth and multimodal limit states, and simulation failures caused by, e.g., evaluations in the tails of input distributions, pose challenges for RBDO in engineering

Table 2. Reliability formulation RBDO: design variable bounds and optimal designs from MVFOSM, AMV^2+, and FORM methods for MEMS bistable mechanism.

variable/metric				MVFOSM	AMV^2+	FORM
l.b.	name	u.b.	initial $\mathbf{d}^0$	optimal $\mathbf{d}_M^*$	optimal $\mathbf{d}_A^*$	optimal $\mathbf{d}_F^*$
10	$L_1\,(\mu m)$	35	25.0	19.23	28.04	28.06
10	$L_2\,(\mu m)$	35	25.0	28.44	24.42	24.45
10	$L_3\,(\mu m)$	35	25.0	14.44	30.58	30.68
10	$L_4\,(\mu m)$	35	25.0	35.00	30.55	30.66
0	θ_1 (deg.)	5	1.0	2.733	4.200	4.189
0	θ_2 (deg.)	5	3.0	2.260	2.481	2.488
0	θ_3 (deg.)	5	3.0	2.719	2.465	2.478
0	θ_4 (deg.)	5	1.0	3.230	2.384	2.390
1	$W_0\,(\mu m)$	3	1.7	1.058	1.355	1.346
1	$W_1\,(\mu m)$	3	1.2	2.038	1.275	1.265
2	$W_2\,(\mu m)$	5	3.2	2.390	3.481	3.488
1	$W_3\,(\mu m)$	3	1.2	1.312	2.006	2.004
1	$W_4\,(\mu m)$	3	1.7	1.000	1.333	1.333
	$\mathrm{E}[F_{min}]\ (\mu N)$		-26.29	-5.896	-6.188	-6.292
2	β		5.376	2.000	1.998	1.999
50	$\mathrm{E}[F_{max}]\ (\mu N)$	150	68.69	50.01	57.67	57.33
	$\mathrm{E}[E_2]\ (\mu m)$	8	4.010	5.804	5.990	6.008
	$\mathrm{E}[S_{max}]$ (MPa)	1200	470	1563	1333	1329
	AMV^2+ verified β		3.771	1.804	-	-
	FORM verified β		3.771	1.707	1.784	-

applications, and must be mitigated through a combination of algorithm research, problem formulation, and simulation refinement.

To evaluate the probability-based optimization formulation in Eq. 27, the optimal design $\mathbf{d}_M^*$ from the reliability-based design optimization with MVFOSM (Table 2) is selected as an initial iterate. As indicated in Table 3, this design has $P(-6.2 \leq F_{min} \leq -5.0)$ equal to 0.71 for first-order integration (FORM) or 0.78 for second-order integration (SORM). The goal is to determine if local changes in the design can increase the probability. Optimal designs for this formulation resulting from RBDO with MVFOSM and AMV^2+ using first-order probability integrations are shown in Table 3. The optimization processes both yield designs with increased interval probability (regardless of choice of probability calculation method). However, the initial and optimal design variables only differ slightly in each case. This small design change can be explained by the fact that the chosen initial iterate is already a variance-minimizing design with respect to $\bar{F}_{min} = -5.0$, so the probability formulation essentially recenters the output distribution within the specified interval (from mean at -5.9 and $\beta_{ccdf} = 2$ to mean at -5.5 and balanced tails at -6.2 and -5.0) to achieve maximal interval probability. This is reflected in Table 3, where $F_{min}(\mu_{\mathbf{x}})$ is larger for the optimal designs. Initial studies involving optimization with the β formulation (Eq. 28) did not yield any further improvement in the device's probabilistic performance.

Analysis of the AMV^2+ optimal design ($\mathbf{d}_A^*$ in Table 2) further contrasts the probability and reliability formulations. For this reliability formulation optimal design, $\mathrm{E}[F_{min}] \approx -6.2$ and two input standard deviations separate its mean from -5.0, yet the $P(-6.2 \leq F_{min} \leq -5.0)$ is verified to be 0.47 (AMV^2+ or FORM) or 0.48 (SORM). This design is reliable, but is far from optimal with regard to the probability metric. When $\mathbf{d}_A^*$ is used as an initial iterate in the probability-based formulation, neither of the methods yield a design with higher probability than those reported in Table 3. If controlling the left half of the output distribution were truly important in the reliability context (i.e., if it were unacceptable to have many $-5.0\,\mu N$ devices actuate with force greater than $-6.2\,\mu N$), the combined RIA/PMA formulation discussed in Section IV.A should be considered.

In Table 3 there is substantial difference between the verified probabilities using first and second-order

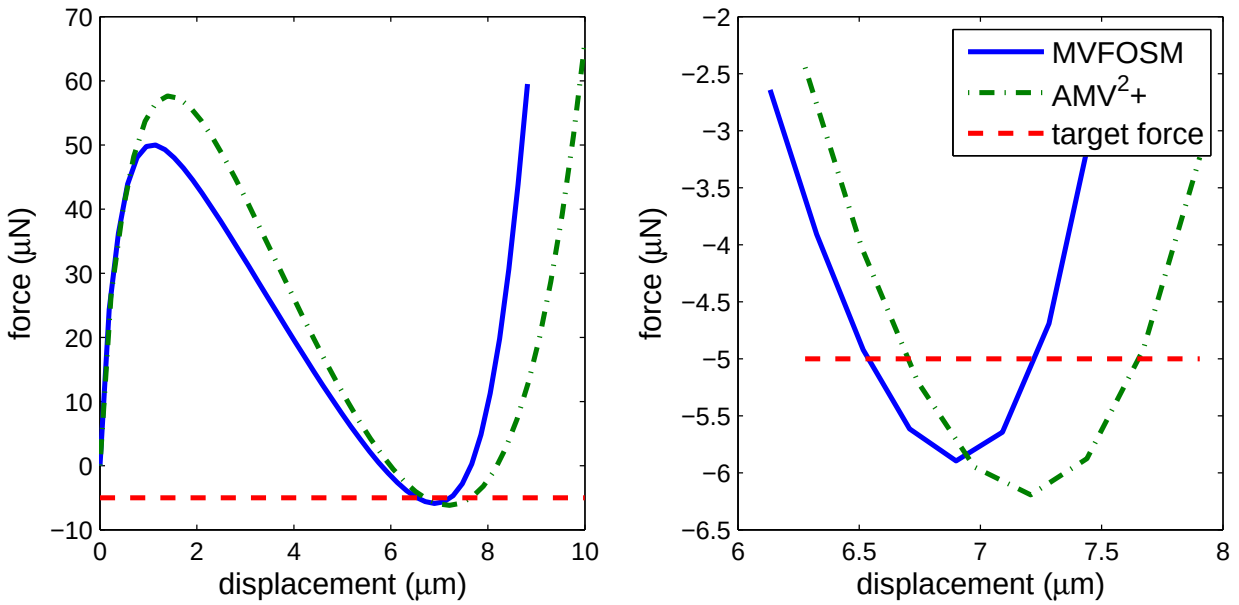

Figure 6. Optimal force–displacement curves resulting from RBDO of MEMS bistable mechanism with mean value and AMV^2+ methods. The right plot shows the area near the minimum force. Two input standard deviations (as measured by the method used during optimization) separate F_{min} from the target $\bar{F}_{min} = -5.0$.

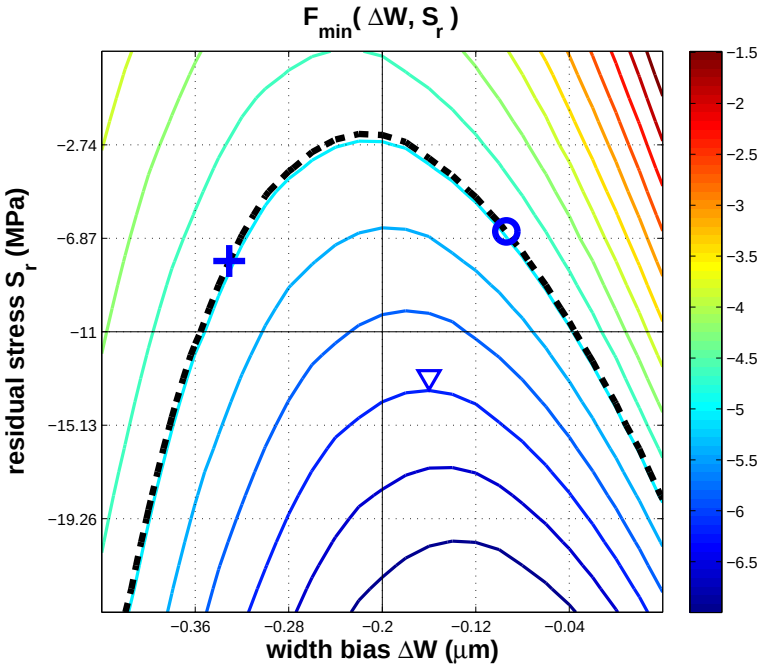

Figure 7. Contour plot of $F_{min}(\mathbf{d}, \mathbf{x})$ as a function of uncertain variables x (design variables d fixed at MVFOSM optimal $\mathbf{d}^*_M$). Dashed line: limit state $g(\mathbf{x}) = F_{min}(\mathbf{x}) = -5.0$; plus sign: MPP from AMV^2+; circle: MPP from FORM; triangle indicates contour corresponding to $F_{min} = -6.2$.

integrations. This observation, in conjunction with the nonlinear limit state plot in Figure 7, motivates higher-order probability integration techniques for use in an RBDO context.

Table 3. Probability formulation RBDO results including MVFOSM and AMV^2+ methods with first-order probability integrations and verified probability with AMV^2+ and FORM (first-order integrations) and SORM (second-order integrations)

variable/metric				MVFOSM	AMV^2+
l.b.	name	u.b.	initial	optimal	optimal
10	$L_1\,(\mu m)$	35	19.23	19.20	19.21
10	$L_2\,(\mu m)$	35	28.44	28.41	28.43
10	$L_3\,(\mu m)$	35	14.44	14.42	14.43
10	$L_4\,(\mu m)$	35	35.00	34.99	35.00
0	θ_1 (deg.)	5	2.733	2.732	2.730
0	θ_2 (deg.)	5	2.260	2.258	2.255
0	θ_3 (deg.)	5	2.719	2.718	2.716
0	θ_4 (deg.)	5	3.230	3.237	3.239
1	$W_0\,(\mu m)$	3	1.058	1.061	1.059
1	$W_1\,(\mu m)$	3	2.038	2.043	2.041
2	$W_2\,(\mu m)$	5	2.390	2.392	2.391
1	$W_3\,(\mu m)$	3	1.312	1.308	1.307
1	$W_4\,(\mu m)$	3	1.000	1.003	1.002
	$P(-6.2 \leq F_{min} \leq -5.0)$		0.729	0.835	0.835
	$F_{min}(\mu_{\mathbf{x}})\,(\mu N)$		-5.896	-5.580	-5.546
50	$\mathrm{E}\left[F_{max}\right]\,(\mu N)$	150	50.01	50.01	49.71
	$\mathrm{E}\left[E_2\right]\,(\mu m)$	8	5.804	5.833	5.835
	$\mathrm{E}\left[S_{max}\right]$ (MPa)	1200	1563	1568	1565
	verified P (AMV^2+)		0.705	0.809	-
	verified P (FORM)		0.713	0.809	0.829
	verified P (SORM)		0.781	0.885	0.858

V. Conclusions

This paper explores the deployment of reliability analysis and design algorithmic capabilities to probabilistic analysis and design of microelectromechanical systems (MEMS). A new bistable switch design is presented and its geometry optimized using DAKOTA in conjunction with Aria, resulting in considerably improved performance. The results include comparison of probability and reliability-based formulations as well as algorithmic variations. Caution is necessary when using uncertainty quantification methods such as mean value that relies on normality or probability integrations that rely on limit state approximations, as they may give false confidence in the reliability of a design.

In performing risk-informed design with computer models, it is crucial to understand the fidelity of the simulation model used. Work is in progress to extend the reliability methods in DAKOTA to leverage error estimates from the finite element analysis codes used to simulate the bistable MEMS. The addition of adjoint computation methods to Aria enables calculation of error estimates on specific quantities of interest output from the simulation. For example, in addition to outputting the required force–displacement curve, the software will output an estimate of the error in the force, indicated by convergence of the finite element solution for the particular finite element mesh used.[40]

Like global error metrics, these error estimates can be used to adaptively refine meshes to ensure solutions sufficiently accurate for the application at hand. However, in contrast to global or norm error estimates, these quantity of interest error estimates also quantify the error in the particular metrics (e.g., force or maximum stress) being used in the optimization and reliability problems. They offer promise for both correcting outputs of numerical codes and quantifying discretization error to better inform the probabilistic design of engineering systems.

Acknowledgments

The authors thank Brian Carnes, Kevin Copps, Matthew Hopkins, David Neckels, Pat Notz, and Sam Subia for developing nonlinear mechanics and error estimation capability in Aria, and Kendall Pierson for optimizing early Adagio simulations of the bistable mechanism.

References

[1]Allen, J. J., *Micro Electro Mechanical System Design*, Taylor and Francis, Boca Raton, 2005.

[2]Coleman, H. W. and Steele, W. G., *Experimentation and Uncertainty Analysis for Engineers*, Wiley, New York, 2nd ed., 1999.

[3]Saltelli, A., Chan, K., and Scott, E. M., *Sensitivity Analysis*, Wiley, New York, 2000.

[4]Schenato, L., Wu, W. C., Ghaoui, L. E., and Pister, K., "Process Variation Analysis for MEMS Design," *Proc. SPIE*, Vol. 4236, 2001, pp. 272–279.

[5]Haldar, A. and Mahadevan, S., *Probability, Reliability, and Statistical Methods in Engineering Design*, Wiley, New York, 2000.

[6]Wu, Y.-T., Millwater, H. R., and Cruse, T. A., "Advanced Probabilistic Structural Analysis Method for Implicit Performance Functions," *AIAA J.*, Vol. 28, No. 9, 1990, pp. 1663–1669.

[7]Wang, L. and Grandhi, R. V., "Efficient Safety Index Calculation for Structural Reliability Analysis," *Comput. Struct.*, Vol. 52, No. 1, 1994, pp. 103–111.

[8]Xu, S. and Grandhi, R. V., "Effective Two-Point Function Approximation for Design Optimization," *AIAA J.*, Vol. 36, No. 12, 1998, pp. 2269–2275.

[9]Tu, J., Choi, K. K., and Park, Y. H., "A New Study on Reliability-Based Design Optimization," *J. Mech. Design*, Vol. 121, 1999, pp. 557–564.

[10]Allen, M. and Maute, K., "Reliability-based Design Optimization of Aeroelastic Structures," *Struct. Multidiscip. O.*, Vol. 27, 2004, pp. 228–242.

[11]Wu, Y.-T., Shin, Y., Sues, R., and Cesare, M., "Safety-Factor Based Approach for Probability-Based Design Optimization," *Proceedings of the 42rd AIAA/ASME/ASCE/AHS/ASC Structures, Structural Dynamics, and Materials Conference*, No. AIAA-2001-1522, Seattle, WA, April 16–19, 2001.

[12]Du, X. and Chen, W., "Sequential Optimization and Reliability Assessment Method for Efficient Probabilistic Design," *J. Mech. Design*, Vol. 126, 2004, pp. 225–233.

[13]Agarwal, H., Renaud, J. E., Lee, J. C., and Watson, L. T., "A Unilevel Method for Reliability Based Design Optimization," *Proceedings of the 45th AIAA/ASME/ASCE/AHS/ASC Structures, Structural Dynamics, and Materials Conference*, No. AIAA-2004-2029, Palm Springs, CA, April 19–22, 2004.

[14]Liu, R., Paden, B., and Turner, K., "MEMS Resonators that are Robust to Process-induced Feature Width Variations," *J. Microelectromech. Syst.*, Vol. 11, 2002, pp. 505–551.

[15]Mawardi, A. and Pitchumani, R., "Design of Microresonators under Uncertainty," *J. Microelectromech. Syst.*, Vol. 14, 2005, pp. 63–69.

[16]Maute, K. and Frangopol, D. M., "Reliability-based Design of MEMS Mechanisms by Topology Optimization," *Comput. Structures*, Vol. 81, 2003, pp. 813–824.

[17]Wittwer, J. W., Baker, M. S., and Howell, L. L., "Robust Design and Model Validation of Nonlinear Compliant Micromechanisms," *J. Microelectromechanical Sys.*, Vol. 15, No. 1, 2006, to appear.

[18]Eldred, M. S., Giunta, A. A., van Bloemen Waanders, B. G., Wojtkiewicz, Jr., S. F., Hart, W. E., and Alleva, M. P., "DAKOTA, A Multilevel Parallel Object-Oriented Framework for Design Optimization, Parameter Estimation, Uncertainty Quantification, and Sensitivity Analysis. Version 3.1 Users Manual," Tech. Rep. SAND2001-3796, Sandia National Laboratories, Albuquerque, NM, Revised April 2003.

[19]Rosenblatt, M., "Remarks on a Multivariate Transformation," *Ann. Math. Stat.*, Vol. 23, No. 3, 1952, pp. 470–472.

[20]Der Kiureghian, A. and Liu, P. L., "Structural Reliability Under Incomplete Probability Information," *J. Eng. Mech., ASCE*, Vol. 112, No. 1, 1986, pp. 85–104.

[21]Box, G. E. P. and Cox, D. R., "An Analysis of Transformations," *J. Royal Stat. Soc.*, Vol. 26, 1964, pp. 211–252.

[22]Rackwitz, R. and Fiessler, B., "Structural Reliability under Combined Random Load Sequences," *Comput. Struct.*, Vol. 9, 1978, pp. 489–494.

[23]Chen, X. and Lind, N. C., "Fast Probability Integration by Three-Parameter Normal Tail Approximation," *Struct. Saf.*, Vol. 1, 1983, pp. 269–276.

[24]Wu, Y.-T. and Wirsching, P. H., "A New Algorithm for Structural Reliability Estimation," *J. Eng. Mech., ASCE*, Vol. 113, 1987, pp. 1319–1336.

[25]Eldred, M. S., Agarwal, H., Perez, V. M., Wojtkiewicz, Jr., S. F., and Renaud, J. E., "Investigation of Reliability Method Formulations in DAKOTA/UQ," *Structure & Infrastructure Engineering: Maintenance, Management, Life-Cycle Design & Performance*, to appear.

[26]Eldred, M. S. and Bichon, B. J., "New Second-Order Reliability Formulations for Reliability Analysis and Design," in preparation.

[27]Eldred, M. S., Giunta, A. A., Wojtkiewicz Jr., S. F., and Trucano, T. G., "Formulations for Surrogate-Based Optimization Under Uncertainty," *Proceedings of the 9th AIAA/ISSMO Symposium on Multidisciplinary Analysis and Optimization*, No. AIAA-2002-5585, Atlanta, GA, September 4–6, 2002.

[28]Hohenbichler, M. and Rackwitz, R., "Sensitivity and Importance Measures in Structural Reliability," *Civil Eng. Syst.*, Vol. 3, 1986, pp. 203–209.

[29]Karamchandani, A. and Cornell, C. A., "Sensitivity Estimation within First and Second Order Reliability Methods," *Struct. Saf.*, Vol. 11, 1992, pp. 95–107.

[30]Zou, T., Mahadevan, S., and Rebba, R., "Computational Efficiency in Reliability-Based Optimization," *Proceedings of the 9th ASCE Specialty Conference on Probabilistic Mechanics and Structural Reliability*, Albuquerque, NM, July 26–28, 2004.

[31]Eldred, M. S. and Giunta, A. A., "Implementation of a Trust Region Model Management Strategy in the DAKOTA Optimization Toolkit," *Proceedings of the 8th AIAA/USAF/NASA/ISSMO Symposium on Multidisciplinary Analysis and Optimization*, No. AIAA-2000-4935, Long Beach, CA, September 6–8, 2000.

[32]Kemeny, D. C., Howell, L. L., and Magleby, S. P., "Using Compliant Mechanisms to Improve Manufacturability in MEMS," *Proc. 2002 ASME DETC*, No. DETC2002/DFM-34178, 2002.

[33]Ananthasuresh, G. K., Kota, S., and Gianchandani, Y., "A Methodical Approach to the Design of Compliant Micromechanisms," *Proc. IEEE Solid-State Sensor and Actuator Workshop*, Hilton Head Island, SC, 1994, pp. 189–192.

[34]Jensen, B. D., Parkinson, M. B., Kurabayashi, K., Howell, L. L., and Baker, M. S., "Design Optimization of a Fully-Compliant Bistable Micro-Mechanism," *Proc. 2001 ASME Intl. Mech. Eng. Congress and Exposition*, New York, NY, November 11–16, 2001.

[35]Wittwer, J. W., *Simulation-based Design under Uncertainty for Compliant Microelectromechanical Systems*, Ph.D. thesis, Brigham Young University, Salt Lake City, UT, April 2005.

[36]Qiu, J. and Slocum, A. H., "A Curved-beam Bistable Mechanism," *J. Microelectromech. Syst.*, Vol. 13, No. 2, 2004, pp. 137–146.

[37]Edwards, H. C., "Sierra Framework for Massively Parallel Adaptive Multiphysics Application," Tech. Rep. SAND2004-6277C, Sandia National Laboratories, Albuquerque, NM, July 2005.

[38]Vanderplaats Research and Development, Inc., Colorado Springs, CO, *DOT Users Manual, Version 4.20*, 1995.

[39]Cox, S. E., Hart, W. E., Haftka, R., and Watson, L., "DIRECT algorithm with box penetration for improved local convergence," *Proc. 9th AIAA/ISSMO Symposium on Multidisciplinary Analysis and Optimization*, No. AIAA-2002-5581, 2002.

[40]Eldred, M. S., Adams, B. M., Copps, K. D., Carnes, B., Notz, P. K., Hopkins, M. M., and Wittwer, J. W., "Solution-Verified Reliability Analysis and Design of Compliant Micro-Electro-Mechanical Systems," *Proceedings of the 9th AIAA Non-Deterministic Approaches Conference*, Honolulu, HI, April 23–26, 2007, in preparation.